Carbon dioxide is, unlike mercury, easy to be dissolved in water and does not easily pass through the ground. Therefore in those places where large amount of underground water is, carbon dioxide distribution may not show geothermal reservoir but only near surface geological structure.

3-2 Interpretation

The result of the survey is shown in the following tables and figures.

(i) Tables of concentration of each element in three survey lines, table III-1 to table III-3

(ii) Maps of horizontal distribution of each element, Fig. III-6 to Fig. III-9

(iii) Sections of three survey lines, Fig. III-10 to Fig. III-12.

Statistical analysis of the data was carried out by an electronics computer and is shown in the following tables and figures.

(i) Elementary statistics, table III-4.

(ii) Mean standard deviation and correlation matrix, table III-5.

(iii) Histogram and cumulative frequency distribution of each element, Fig. III-13 to Fig. III-21

Correlation coefficients between carbon dioxide content and mercury content in soil air and 1 meter depth ground temperature are very high (see Table III-5).

On 1 meter depth temperature map (Fig. III-8), very high temperature (about $90^{o}C$) was measured at two places, the one at A line No. 22.5 and the other at B line No. 17.5. High temperature zones run approximately north to south and are centered at the above mentioned very high temperature points. The high temperature zones coincide their distribution with high anomaly of mercury content and carbon dioxide in soil air (Fig. III-6, Fig. III-7, Fig. III-8). Around the anomalous zones, there are geological alteration zones. Both statistical approach and visual approach show very close correlation of 1 m depth ground temperature, carbon dioxide content and mercury content in soil air.

The maximum values of mercury content in soil air and carbon dioxide content in soil air are 10.5 ng/l (1.05×10^{-11} g/cc) and 55% respectively. 1.05×10^{-11} g/cc of mercury content in soil air is 10^{4} times of normal mercury content and 55%

of carbon dioxide in soil air is over 10^4 times of normal carbon dioxide content in air (0.04%).

Cumulative frequency distribution figures of mercury content in soil air and carbon dioxide content in soil air show that cumulative distribution curves consist of two straight lines. It means these data were taken from two populations, the one background population and the one high anomalous population.

Mercury concentration in soil does not have good correlation with other measurements in correlation matrix table (Table III-5). However, the map of Hg concentration in soil (Fig. III-9) shows high anomaly at around A line No. 22.5, which extend to south, corresponding to high anomaly on Hg concentration in soil air and 1 meter depth ground temperature.

Table III-1 Geochemical Results of A Line

Eburru - A Line

Sample No.	In soil air		In soil *	Temperature 1 m depth in the ground (°C)	Remark
	CO_2 (%)	Hg (ng/l)	Hg (μg/g)		
A - 10	0.4	N.D	2.5	34.0	Eburru peak.
11	1.0	0.75	1.3	37.0	near the alteration zone
12	1.5	0.40	1.1	42.8	
13	3.0	0.25	1.9	28.0	
14	1.0	0.25	0.4	22.7	
15	0.4	N.D	0.5	17.9	
16	0.4	N.D	1.3	21.1	
16.5	0.5	0.10	0.4	19.6	
17	0.6	N.D	0.3	29.5	
17.5	1.6	2.00	1.7	26.5	caldera
18	2.2	0.90	0.4	27.6	
18.5	1.3	0.40	0.2	26.5	
19	0.7	0.25	0.4	25.6	
19.5	1.1	0.75	-	25.5	
20	0.5	N.D	0.8	20.8	
20.5	0.7	N.D	0.3	21.0	
21	0.7	0.15	0.9	20.2	
21.5	0.9	0.30	1.7	22.0	
22	20.0	0.75	0.8	49.0	alteration zone and hot spot
22.5	55.0	10.50	2.0	91.0	
23	6.7	2.00	2.1	56.5	
23.5	0.8	1.05	1.1	39.4	
24	0.5	1.10	1.1	32.3	
24.5	0.9	0.20	0.9	32.6	
25	0.6	0.20	0.1	23.0	
25.5	1.3	1.15	0.3	29.6	
26	1.0	0.40	2.5	34.0	
27	0.3	N.D	0.1	21.5	
28	0.2	N.D	0.1	17.0	forest
29	0.2	N.D	0.1	16.1	caldera basin
30	0.5	N.D	0.9	17.0	

N.D : not detected.

* : analyzed by Mines and Geological Department of Kenya.

Table III-2 Geochemical Results of B Line

Eburru - B Line

Sample No.	In soil air		In soil *	Temperature 1 m depth in the ground (°C)	Remark
	CO_2 (%)	Hg (ng/l)	Hg (μg/g)		
B - 15	1.0	N.D	0.1	23.5	
16	0.9	N.D	0.3	23.0	
16.5	0.2	N.D	0.1	25.6	
17	0.5	0.50	0.9	27.6	
17.5	1.2	0.75	3.9	34.4	↑ alteration and steaming ground
18	7.5	1.75	1.8	50.0	↓
18.5	35.0	6.50	0.2	89.5	
19	0.6	0.25	4.4	29.0	
19.5	1.5	0.25	3.4	41.0	
20	16.6	0.75	3.1	34.4	
20.5	0.6	0.20	1.1	21.1	
21	0.7	N.D	0.9	25.0	
21.5	0.7	0.25	0.9	30.3	
22	7.0	1.25	3.8	63.0	↑ alteration zone
22.5	1.6	0.25	5.8	30.8	↓
23	0.9	0.25	3.5	29.8	
23.5	0.4	N.D	0.8	25.5	
24	0.7	0.15	1.6	30.8	
24.5	1.5	0.25	1.6	33.5	
25	3.5	0.25	6.7	35.0	

Table III-3 Geochemical Results of C Line

Eburru - C Line

Sample No.	In soil air		In soil *	Temperature 1 m depth in the ground (°C)	Remark
	CO_2 (%)	Hg (ng/l)	Hg (μg/g)		
15	0.2	N.D	0.1	17.5	
16	0.3	N.D	0.1	21.5	
16.5	0.3	N.D	0.1	21.5	
17	1.0	N.D	0.1	21.8	
17.5	0.5	0.50	0.1	18.0	
18	0.9	0.60	0.1	23.5	
18.5	0.5	0.50	0.6	22.7	
19	0.5	N.D	0.1	22.0	
19.5	0.9	N.D	0.1	21.6	
20	0.8	N.D	0.1	21.7	
20.5	0.5	N.D	0.1	19.1	
21	0.7	N.D	0.1	21.5	
21.5	1.0	0.40	0.1	27.4	
22	2.4	0.80	1.9	30.0	
22.5	1.6	0.15	1.3	29.6	
23	2.6	0.60	0.6	34.5	
23.5	2.2	0.35	0.1	30.4	
24	0.5	N.D	0.1	25.0	
24.5	0.8	N.D	0.1	28.5	
25	0.7	N.D	0.1	23.7	

Table III-4 Elementary Statistics

* COUNT OF OBSERVATIONS SELECTED (TG>0) : NOS = 70
COUNT OF OBSERVATIONS ON "AOF" FILE : NAOF = 71

	CO2	HG-AIR	HG-SOIL	TEMP(C)
X.MAX(I) =	55.000	10.500	6.700	91.000
X.MIN(I) =	0.200	0.0	0.100	16.100
SUM =	208.000	41.350	79.100	2111.300
CNT.D =	71	71	70	71
MEAN =	2.930	0.582	1.130	29.737
V.BAR =	0.6503D 02	0.2173D 01	0.1925D 01	0.1876D 03
S.D. =	8.064	1.474	1.387	13.696
SD/M =	2.753	2.531	1.228	0.461
V.NEUMANN'S R. =	1.434	1.613	1.270	1.028
SKEWNWSS =	4.973	5.321	1.973	2.776
KURTOSIS =	26.233	30.503	4.044	9.028

* COUNT OF OBSERVATIONS SELECTED (TG>0) : NOS = 70
COUNT OF OBSERVATIONS ON "AOF" FILE : NAOF = 71

	L.CO2	C.L.HA	L.HG-S	L.TP
X.MAX(I) =	1.740	1.021	0.826	1.959
X.MIN(I) =	-0.699	-1.144	-1.000	1.207
SUM =	0.684	-44.263	-19.812	102.444
CNT.D =	71	71	70	71
MEAN =	0.010	-0.623	-0.283	1.443
V.BAR =	0.2403D 00	0.2772D 00	0.3403D 00	0.2283D-01
S.D. =	0.490	0.526	0.583	0.151
SD/M =	50.909	-0.845	-2.061	0.105
V.NEUMANN'S R. =	1.117	0.967	0.947	0.807
SKEWNWSS =	1.520	0.813	0.027	1.309
KURTOSIS =	2.675	0.216	-1.337	2.282

* COUNT OF OBSERVATIONS SELECTED (TG>0) : NOS = 38
COUNT OF OBSERVATIONS ON "AOF" FILE : NAOF = 71

	L.CO2	L.HG-A	C.L.HS	L.TP
X.MAX(I) =	1.740	1.021	0.826	1.959
X.MIN(I) =	-0.699	-1.000	-0.699	1.207
SUM =	0.684	-13.375	2.188	102.444
CNT.D =	71	44	48	71
MEAN =	0.010	-0.304	0.046	1.443
V.BAR =	0.2403D 00	0.1766D 00	0.1486D 00	0.2283D-01
S.D. =	0.490	0.420	0.386	0.151
SD/M =	50.909	-1.383	8.458	0.105
V.NEUMANN'S R. =	1.117	1.496	1.488	0.807
SKEWNWSS =	1.520	1.060	-0.045	1.309
KURTOSIS =	2.675	1.337	-0.682	2.282

Table Ⅲ-5 Mean, Standard Deviation and Correlation Matrix

	MEAN	S.D.	1 CO2	2 HG-AIR	3 HG-SOIL	4 TEMP(C)
1 Z 1 CO2	2.956	8.119	100.0	92.6	12.0	82.9
2 Z 2 HG-AIR	0.580	1.484	92.6	100.0	10.5	83.6
3 Z 3 HG-SOIL	1.130	1.387	12.0	10.5	100.0	32.2
4 Z 4 TEMP(C)	29.797	13.785	82.9	83.6	32.2	100.0

* DEGREE OF FREEDOM : DF = 69.0 SQUARE ROOT OF DF : RDF = 8.3066

	MEAN	S.D.	1 L.CO2	2 L.HG-A	3 C.L.HS	4 L.TP
1 Z 7 L.CO2	0.249	0.525	100.0	69.3	9.5	80.6
2 Z 8 L.HG-A	-0.294	0.446	69.3	100.0	-8.0	75.2
3 Z 13 C.L.HS	0.101	0.389	9.5	-8.0	100.0	16.3
4 Z 10 L.TP	1.523	0.155	80.6	75.2	16.3	100.0

* DEGREE OF FREEDOM : DF = 37.0 SQUARE ROOT OF DF : RDF = 6.0828

	MEAN	S.D.	1 L.CO2	2 C.L.HA	3 L.HG-S	4 L.TP
1 Z 7 L.CO2	0.009	0.494	100.0	75.5	40.9	82.7
2 Z 12 C.L.HA	-0.631	0.527	75.5	100.0	43.7	76.8
3 Z 9 L.HG-S	-0.283	0.583	40.9	43.7	100.0	50.0
4 Z 10 L.TP	1.443	0.152	82.7	76.8	50.0	100.0

* DEGREE OF FREEDOM : DF = 69.0 SQUARE ROOT OF DF : RDF = 8.3066

Fig. Ⅲ - 5 Temperature Variations at Three Different Depth in The Ground and at The Surface.

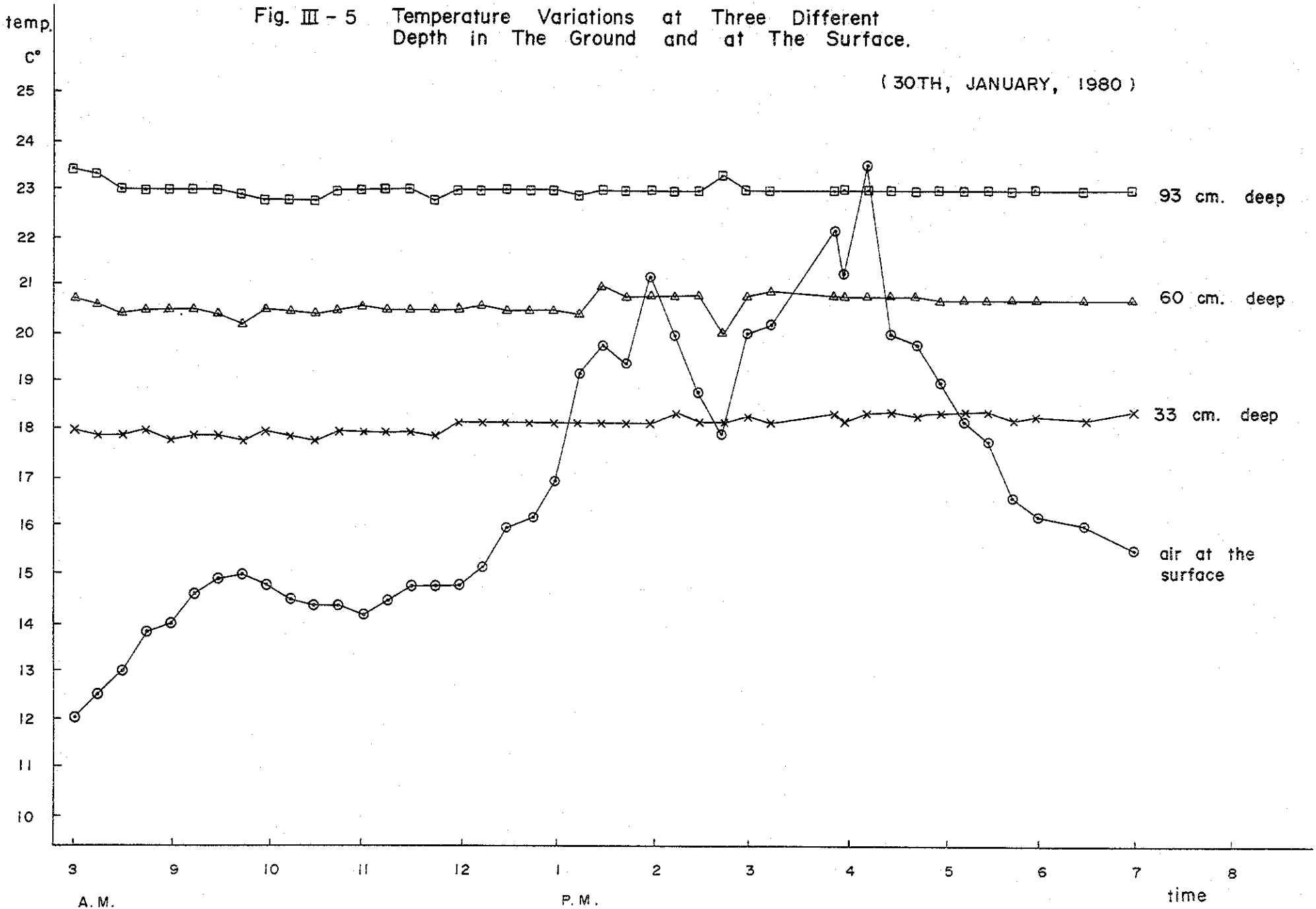

Fig. Ⅲ-6 Hg Concentration in Soil Air

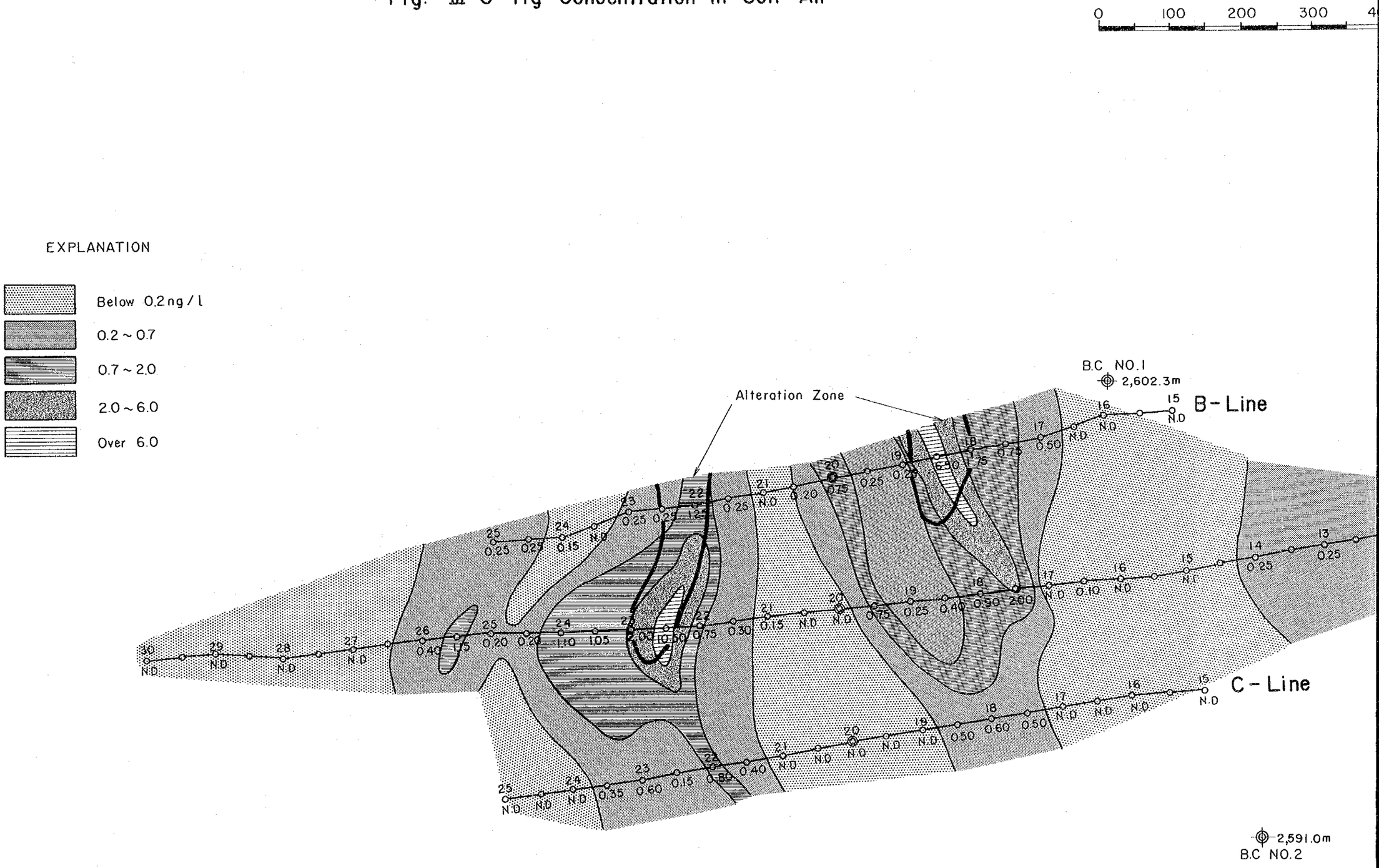

Fig. Ⅲ-6 Hg Concentration in Soil Air

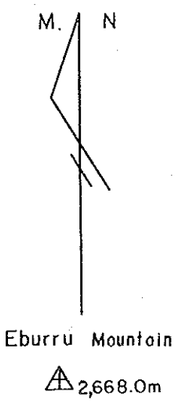

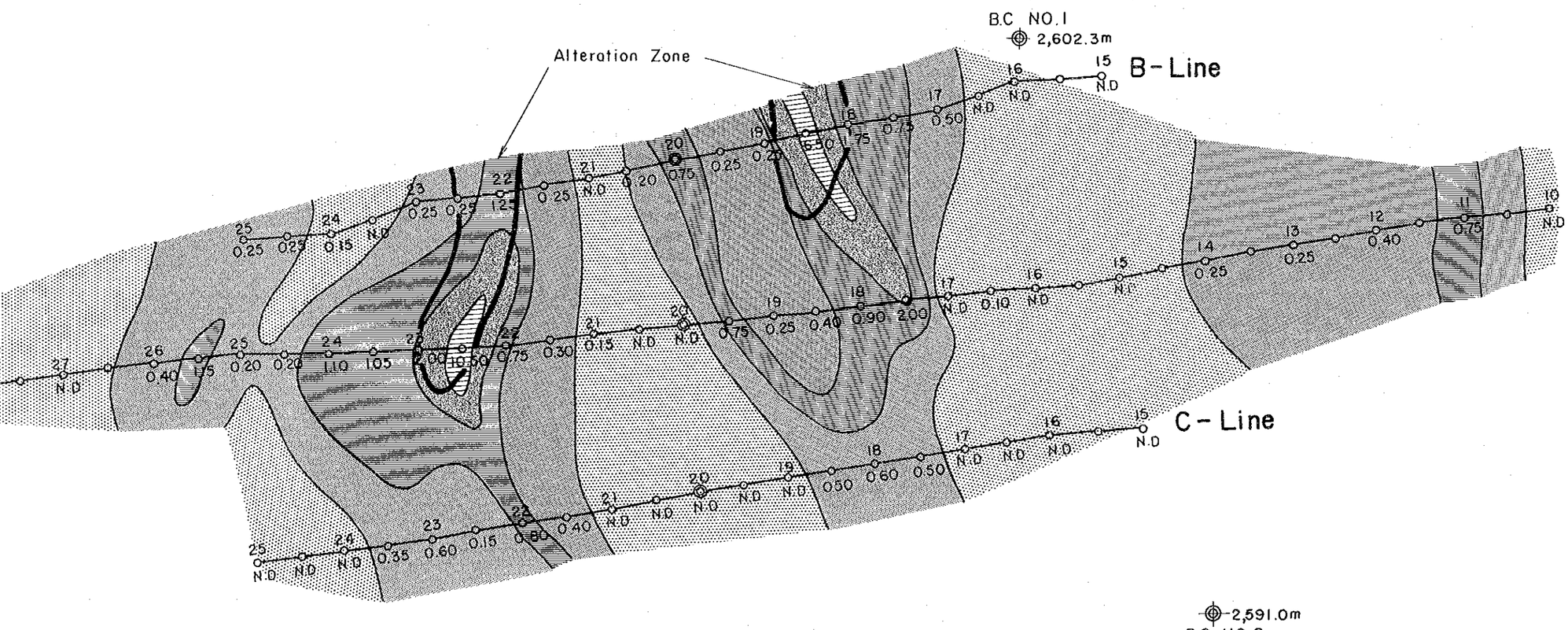

Fig. Ⅲ-7 CO_2 Concentration in Soil Air

0 100 200 300

EXPLANATION

- Below 0.5%
- 0.5 ~ 1.2
- 1.2 ~ 2.0
- 2.0 ~ 4.0
- 4.0 ~ 10.0
- 10.0 ~ 20.0
- Over 20.0

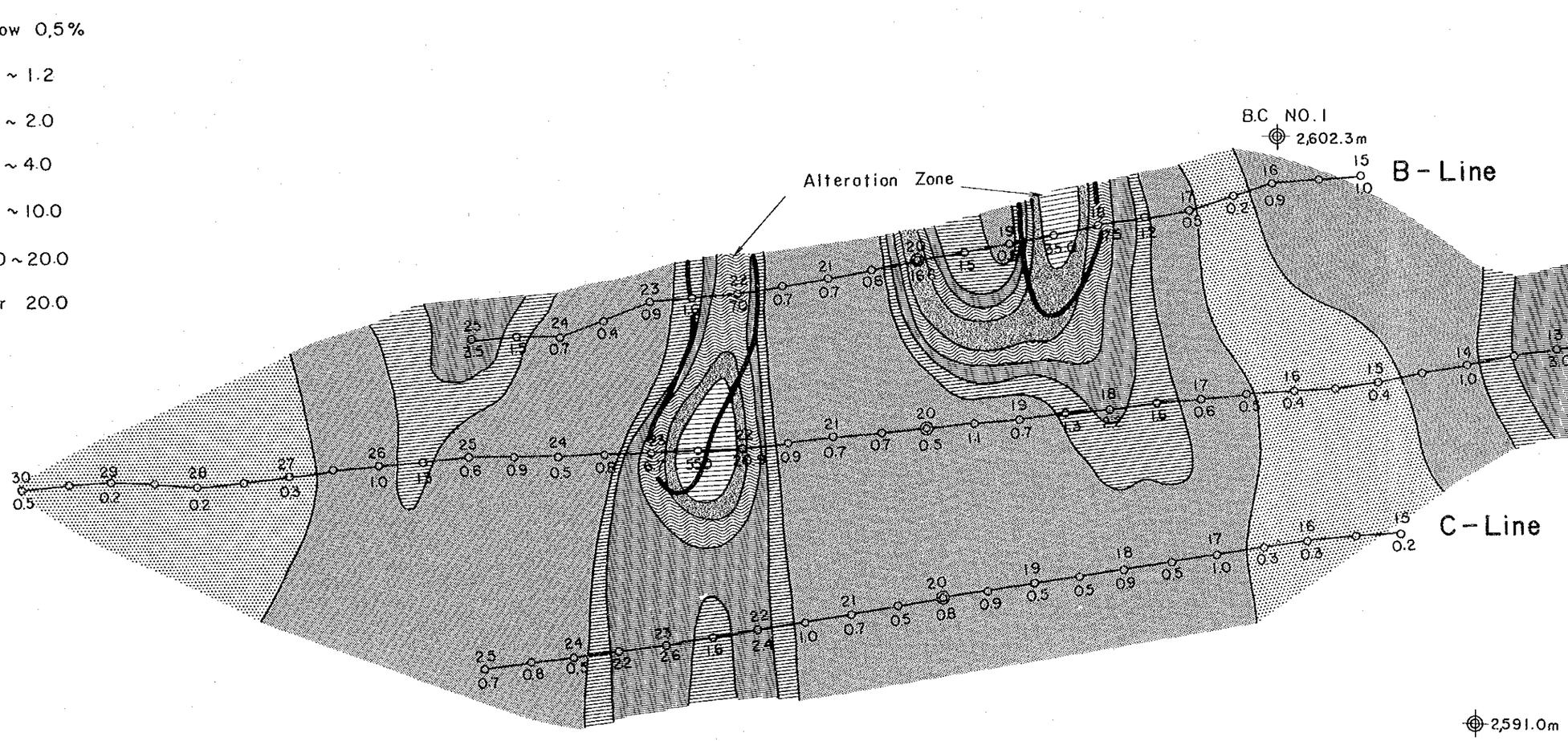

Fig. Ⅲ-7 CO_2 Concentration in Soil Air

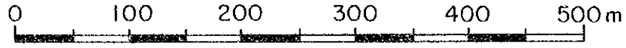

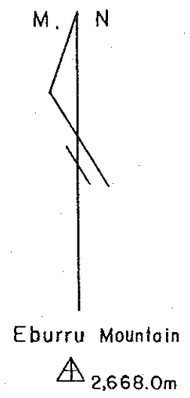

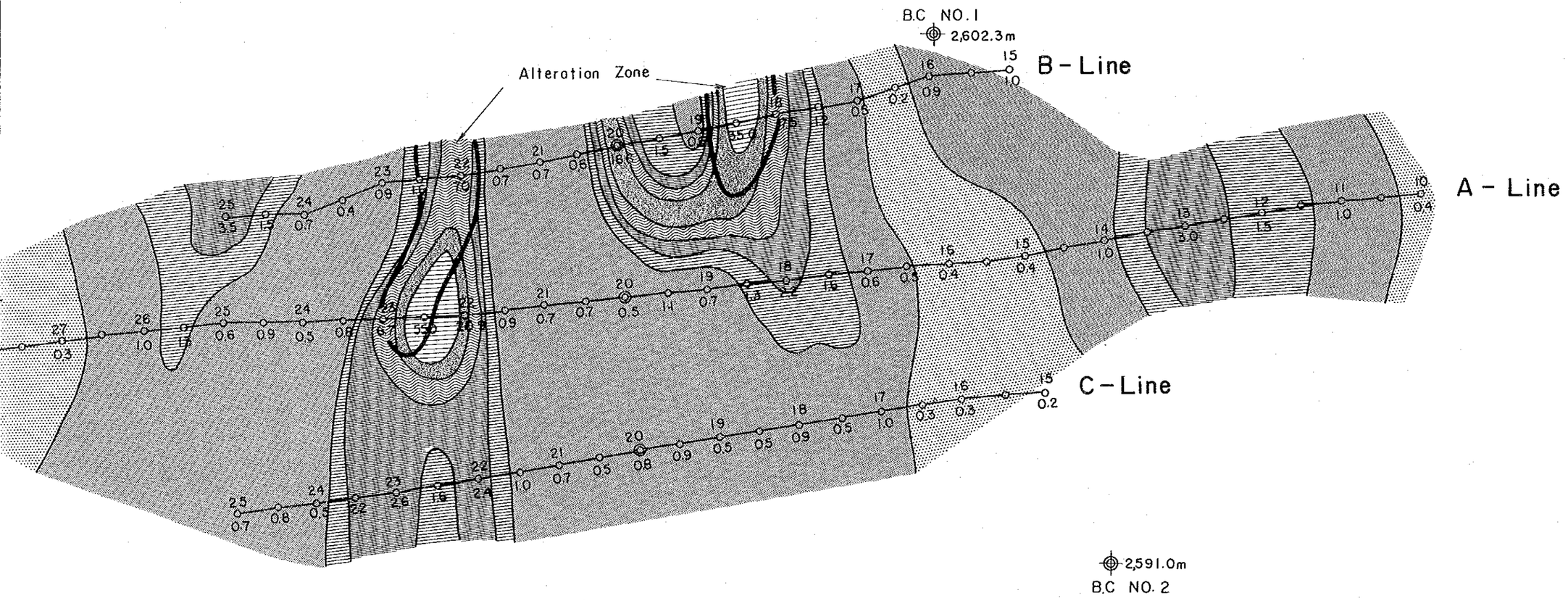

Fig. Ⅲ-8 Temperature of 1m Depth in the Ground

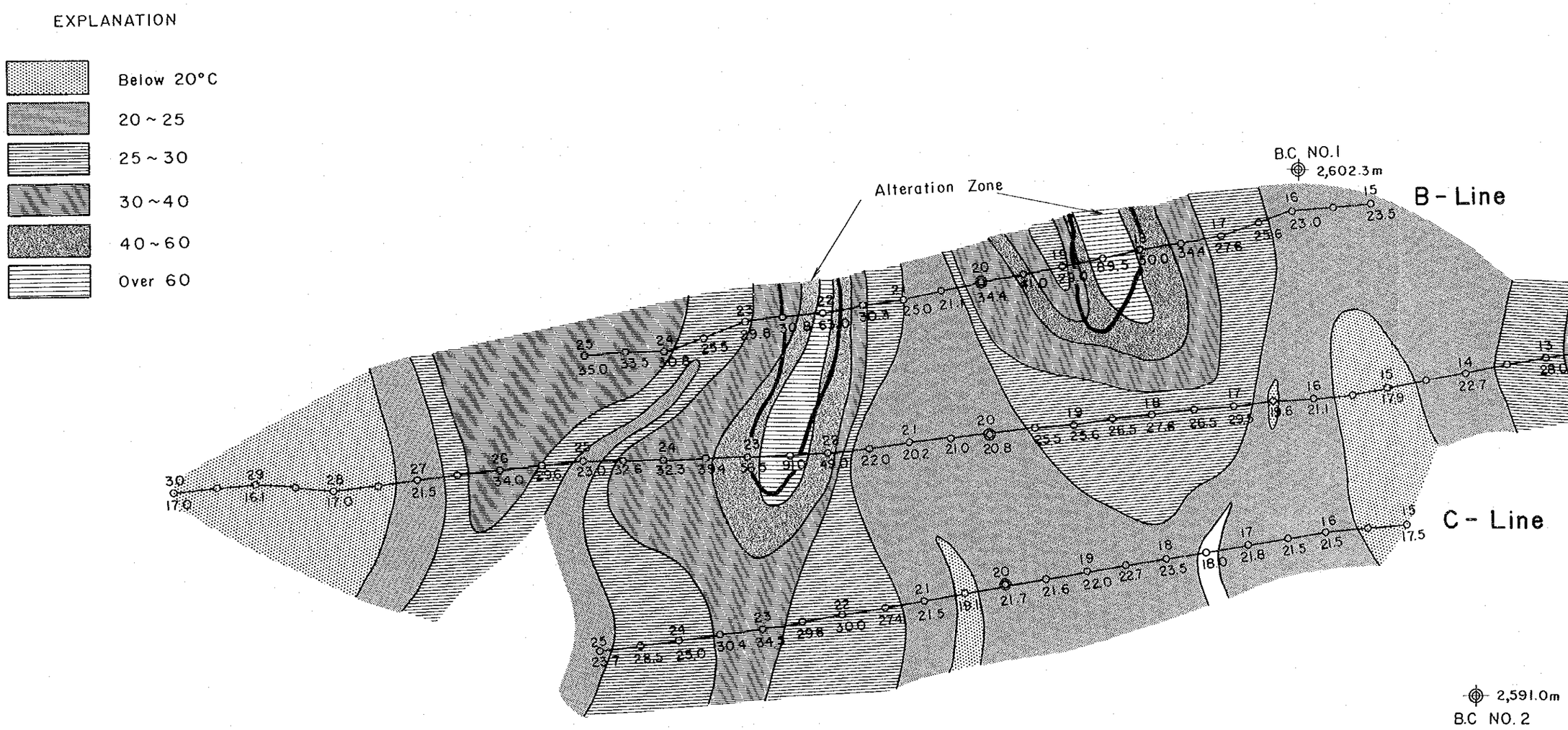

Fig. Ⅲ-8 Temperature of 1m Depth in the Ground

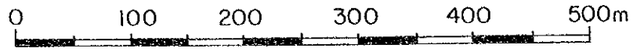

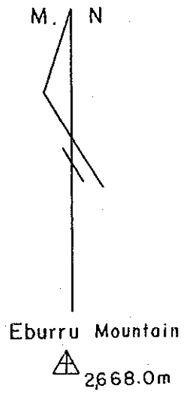

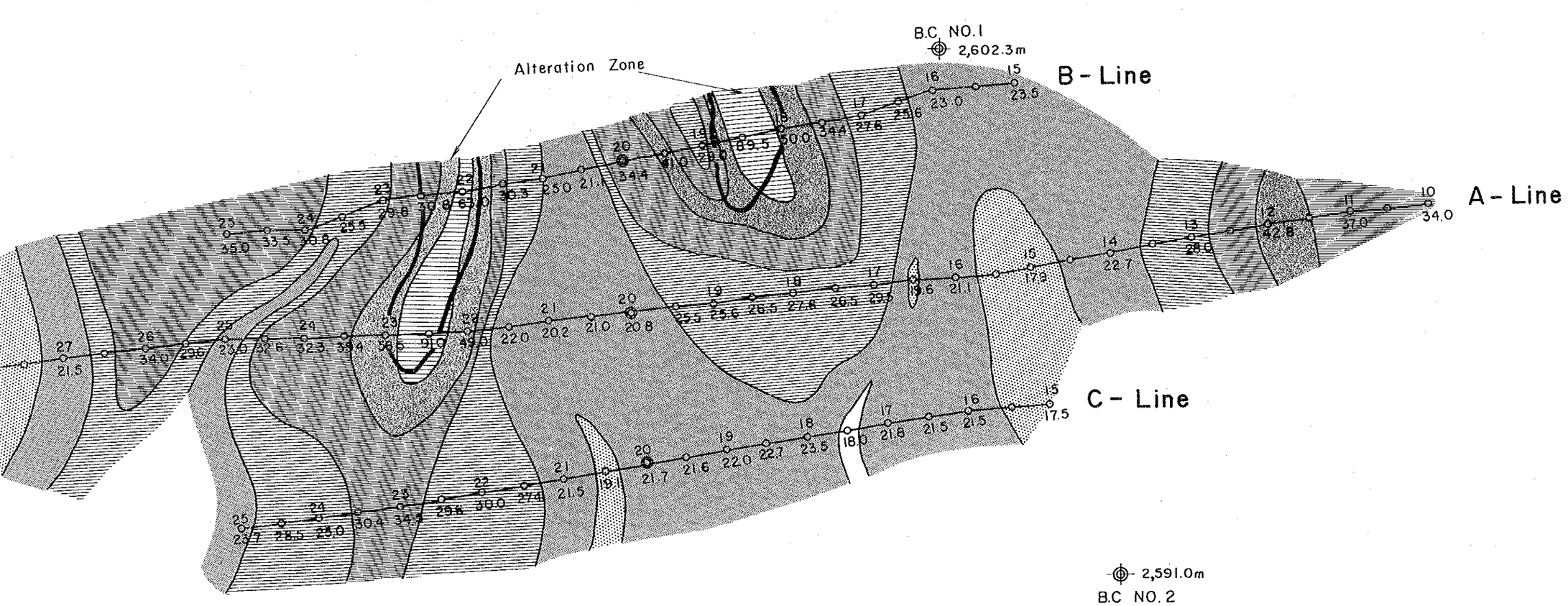

Fig. Ⅲ-9 Hg Concentration in Soil

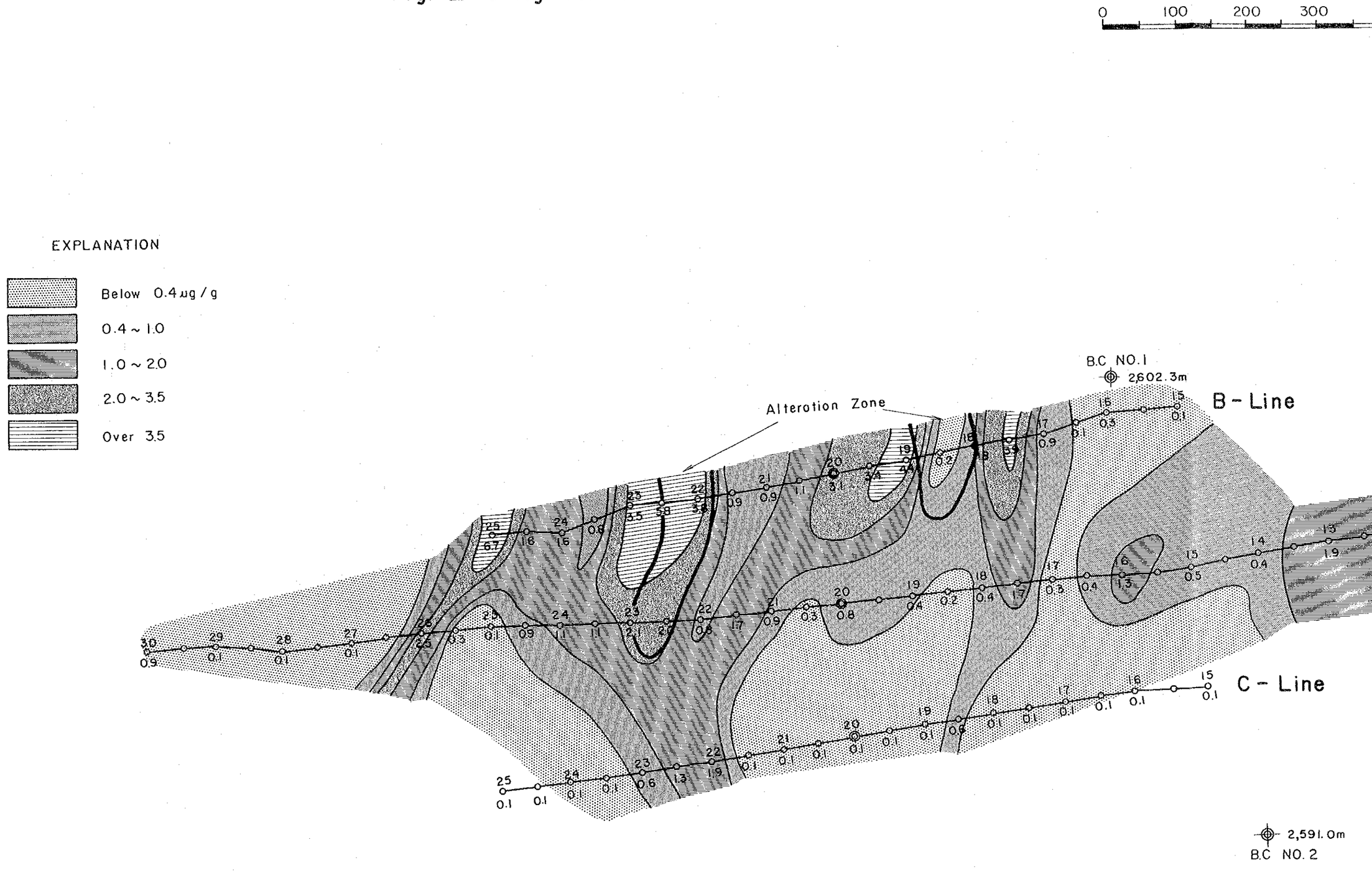

Fig. Ⅲ-9 Hg Concentration in Soil

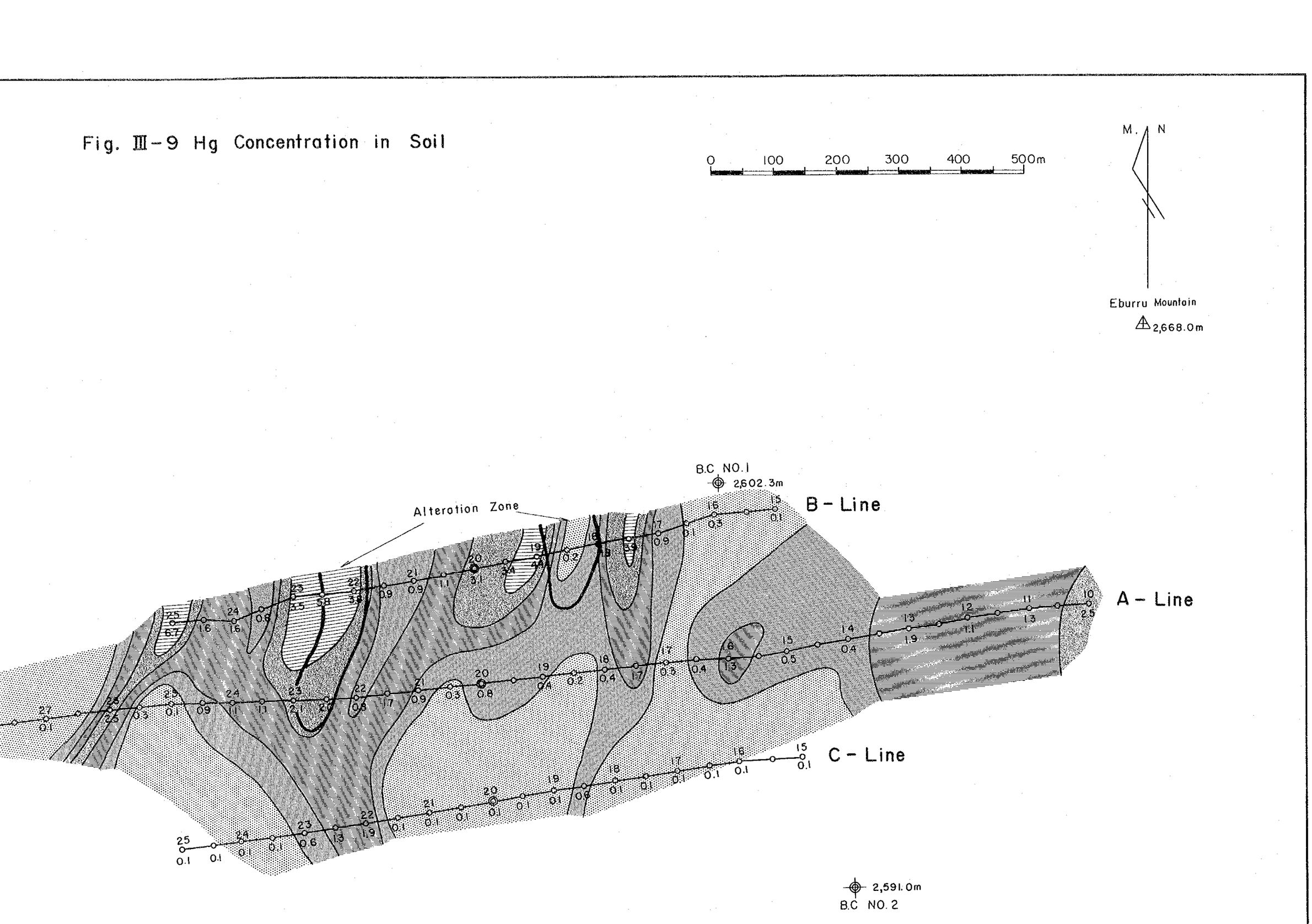

Fig. III-10 Geochemical Results along A Line

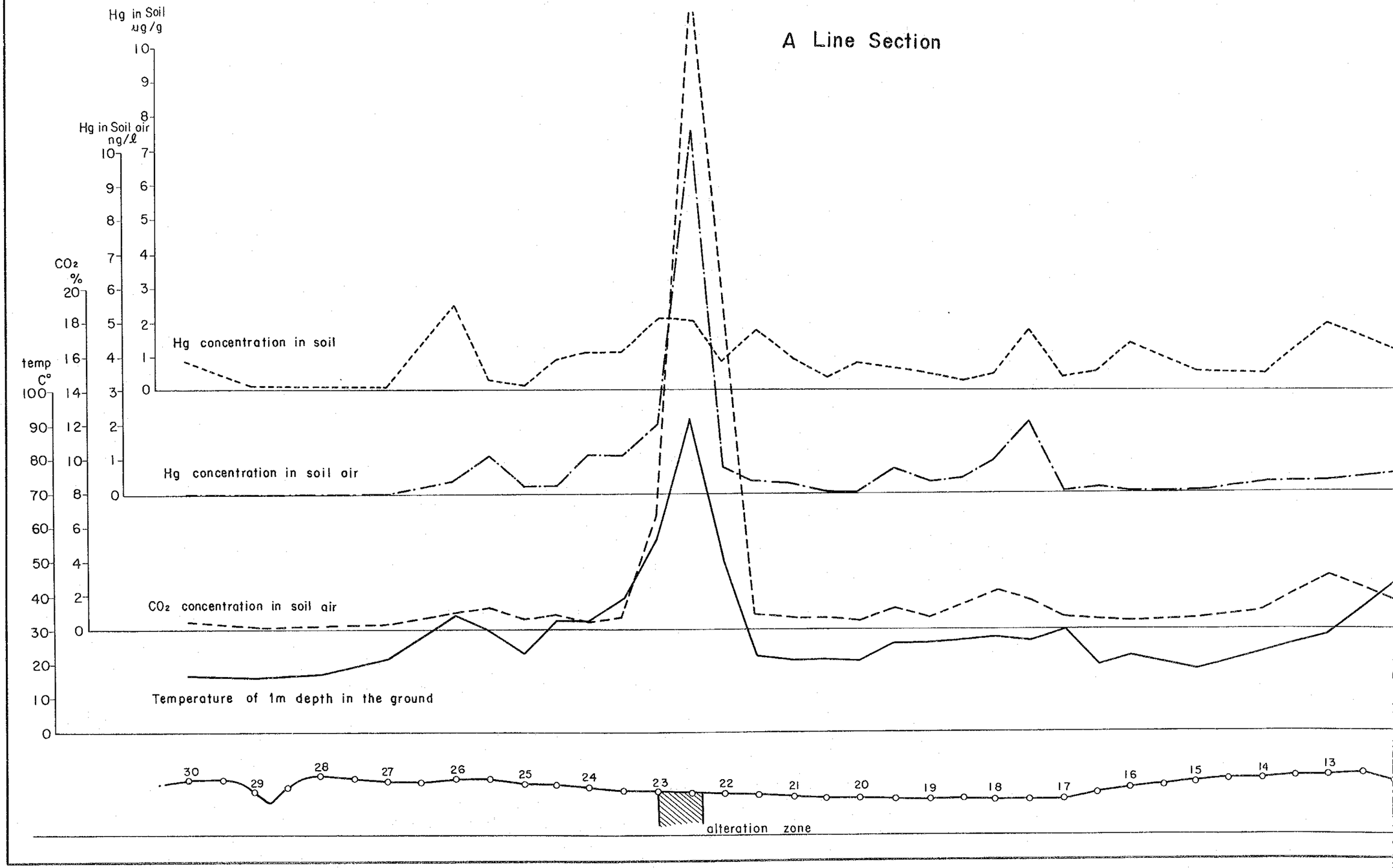

Fig. Ⅲ-10 Geochemical Results along A Line

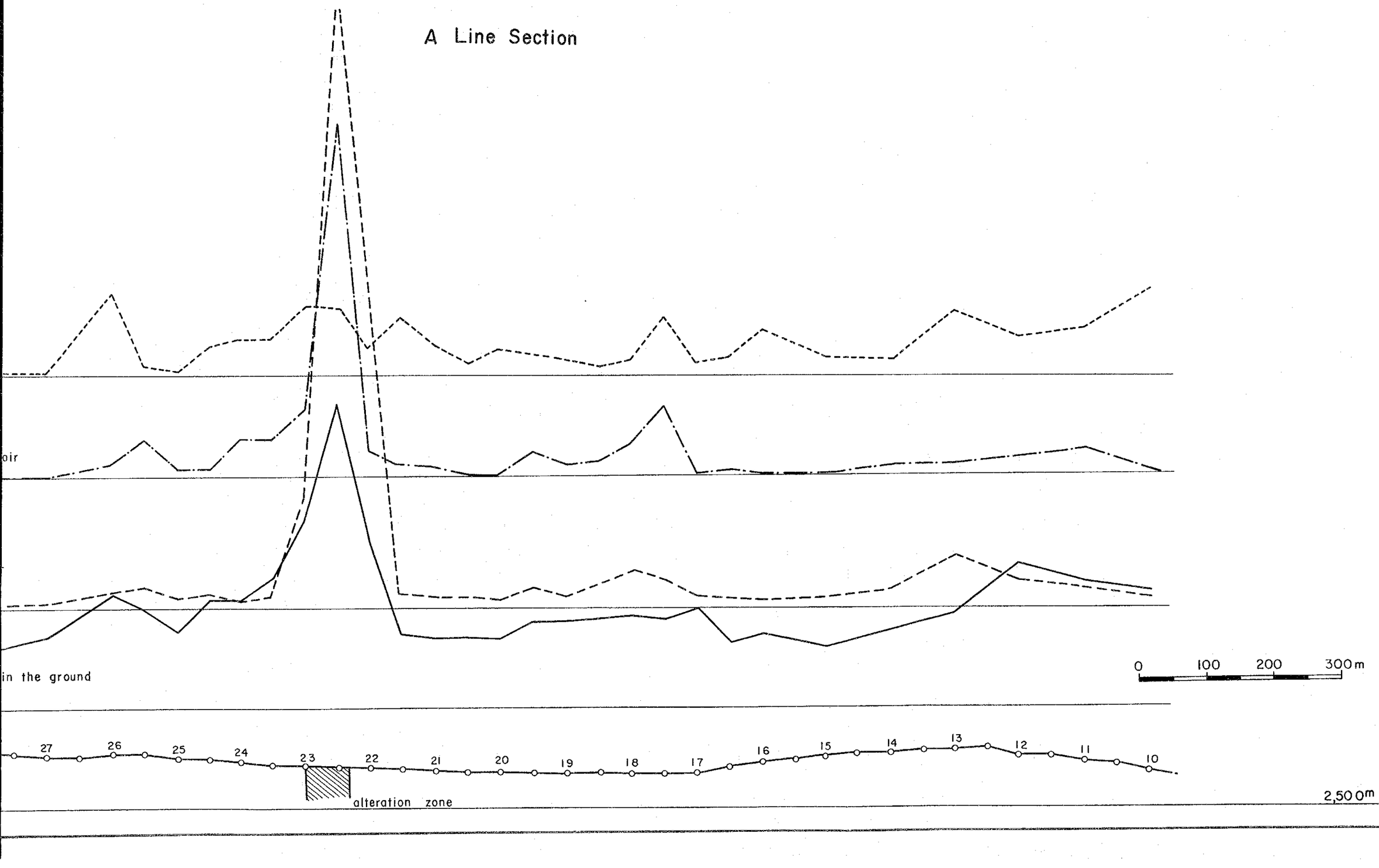

Fig. Ⅲ-11 Geochemical Results along B Line

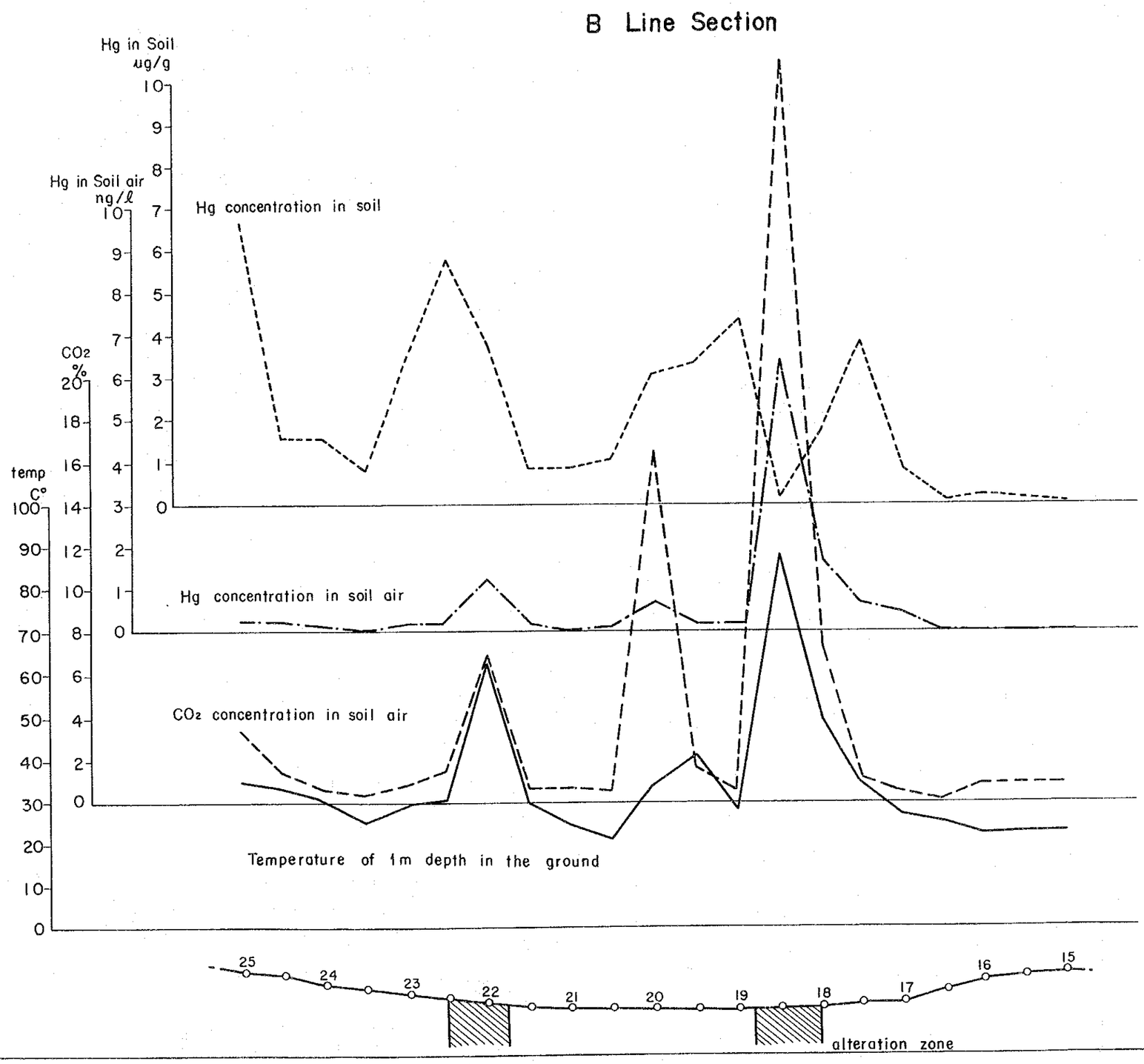

Fig. Ⅲ－11 Geochemical Results along B Line

B Line Section

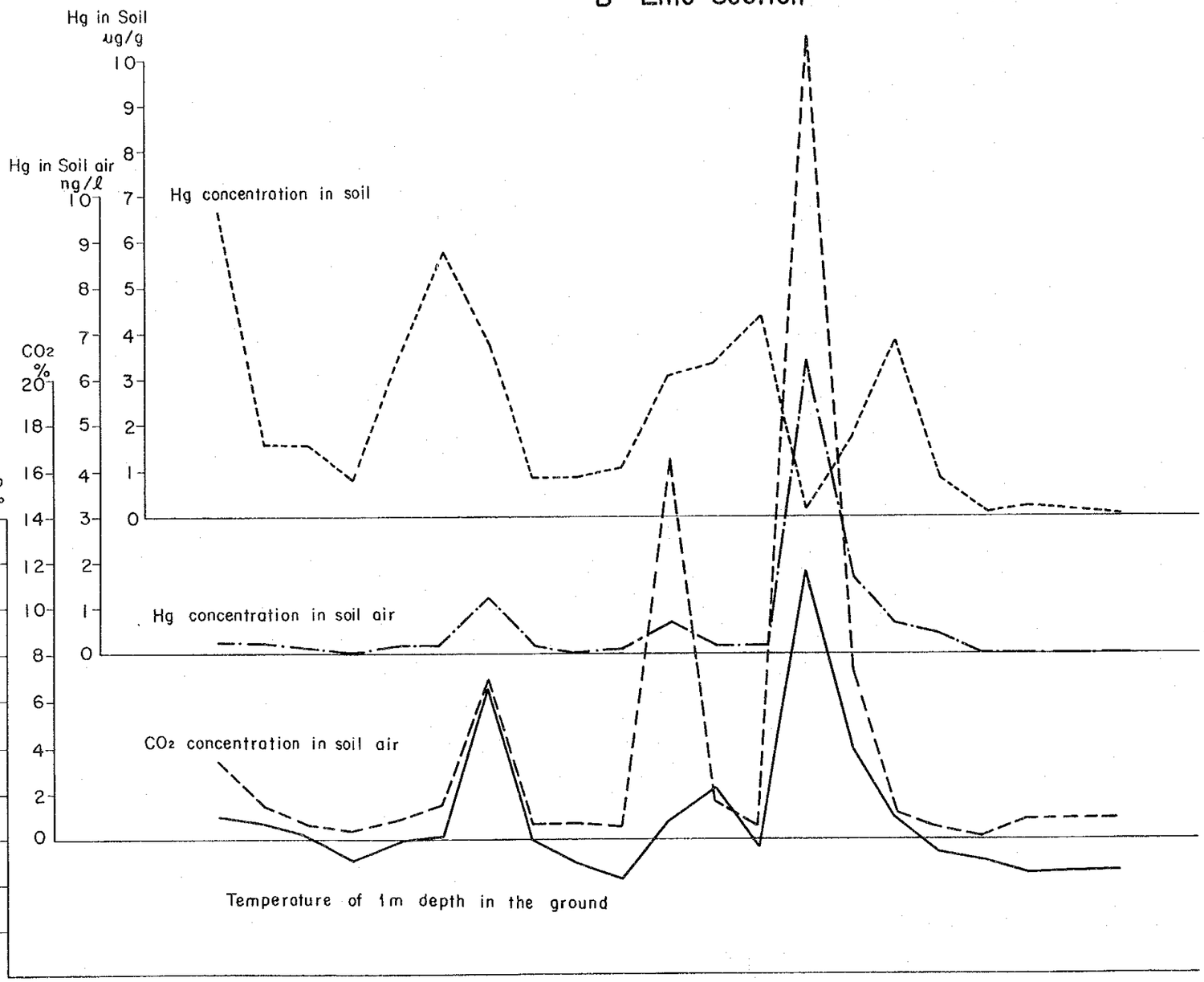

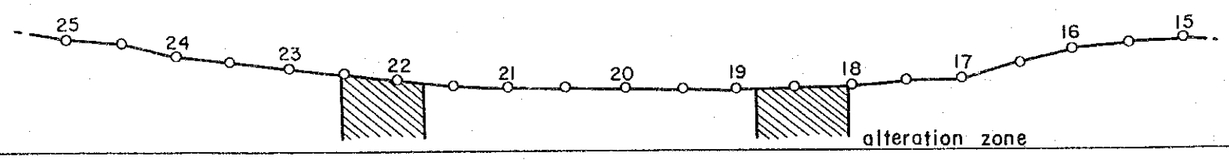

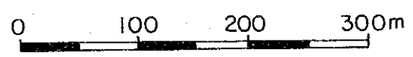

2,500m

Fig. Ⅲ-12 Geochemical Results along C Line

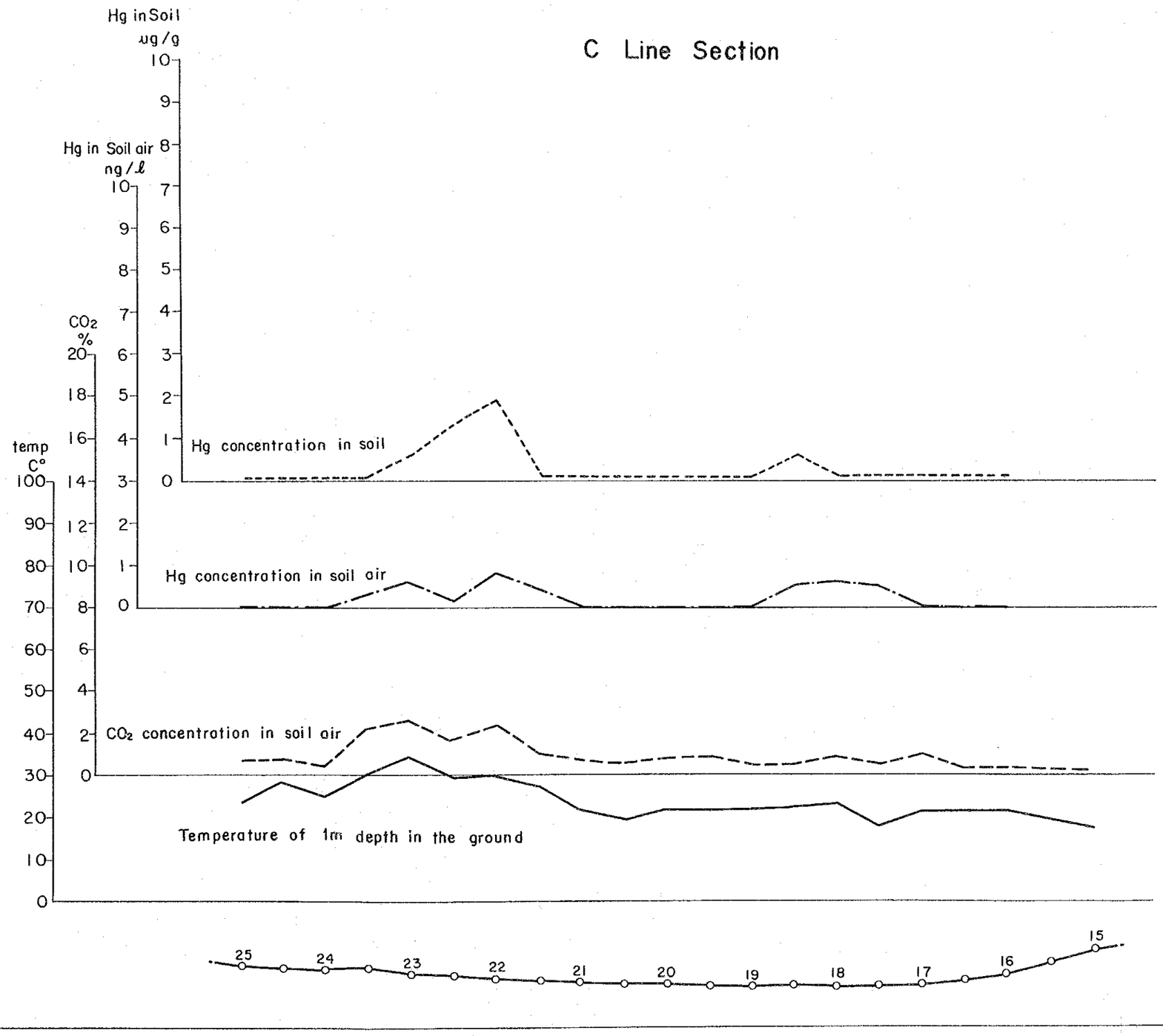

Fig. Ⅲ-12 Geochemical Results along C Line

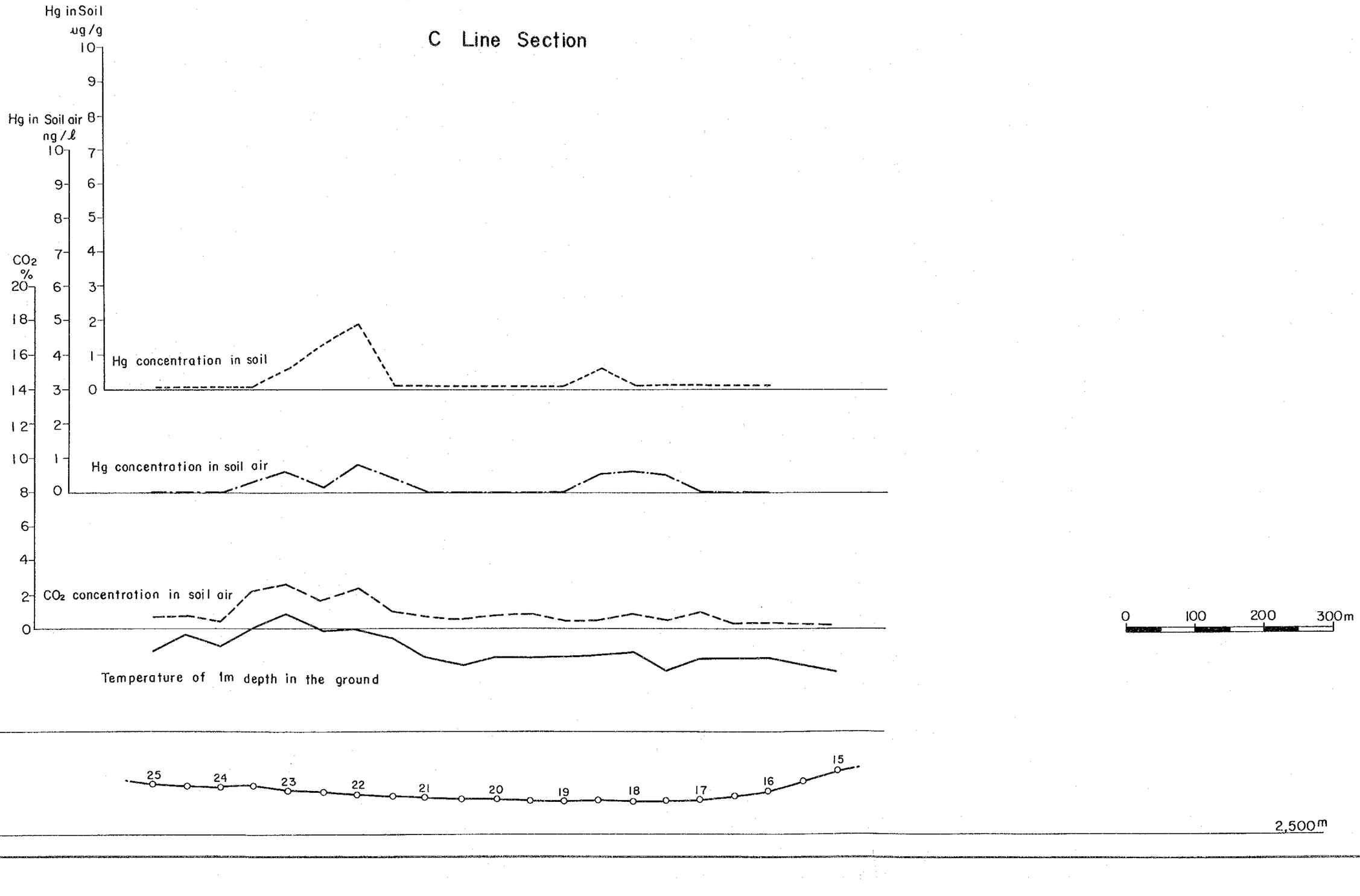

Fig. Ⅲ - 13 TRIANGULAR CHART

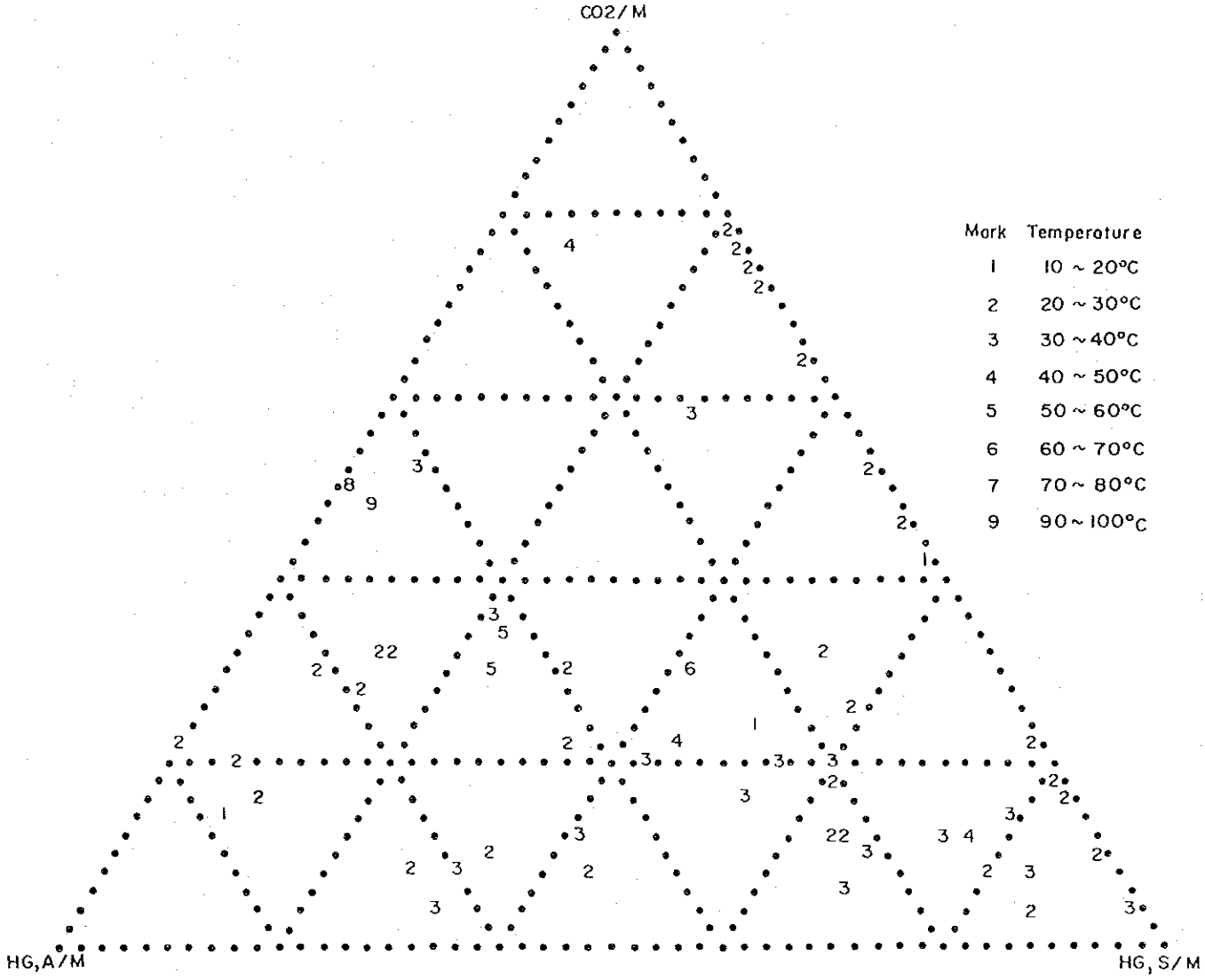

Fig. Ⅲ - 14 HISTOGRAM (HG. Air)

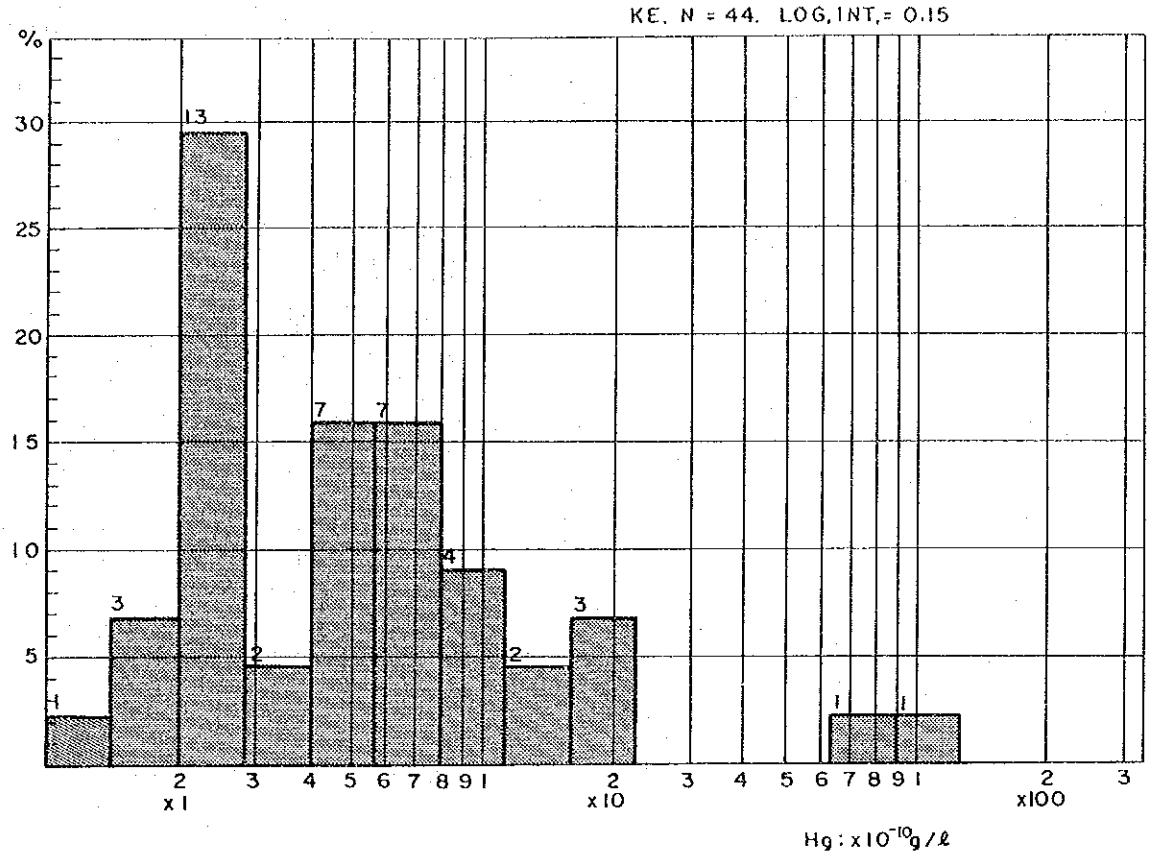

Fig. Ⅲ - 15 CUMULATIVE FREQUENCY DISTRIBUTION (HG. Air)

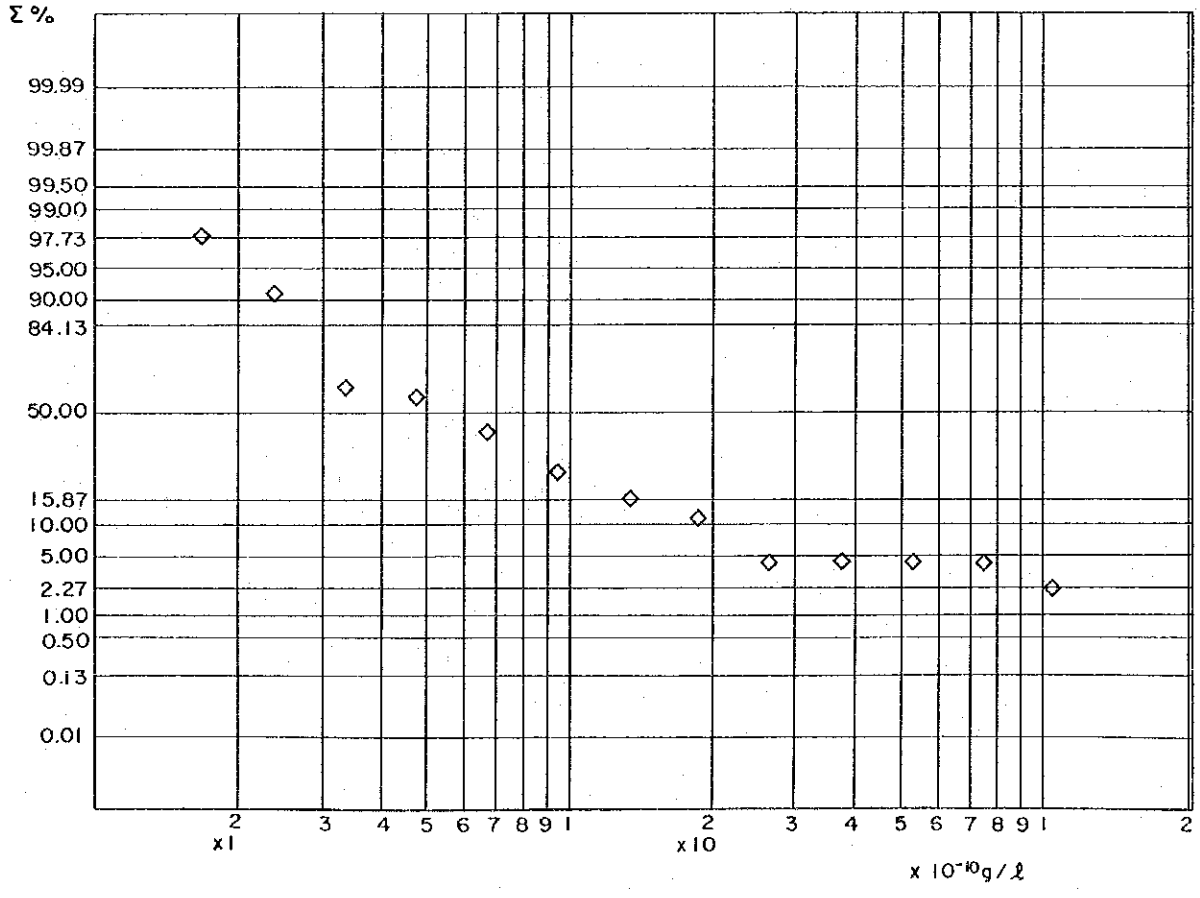

Fig. Ⅲ - 16 HISTOGRAM (CO_2)

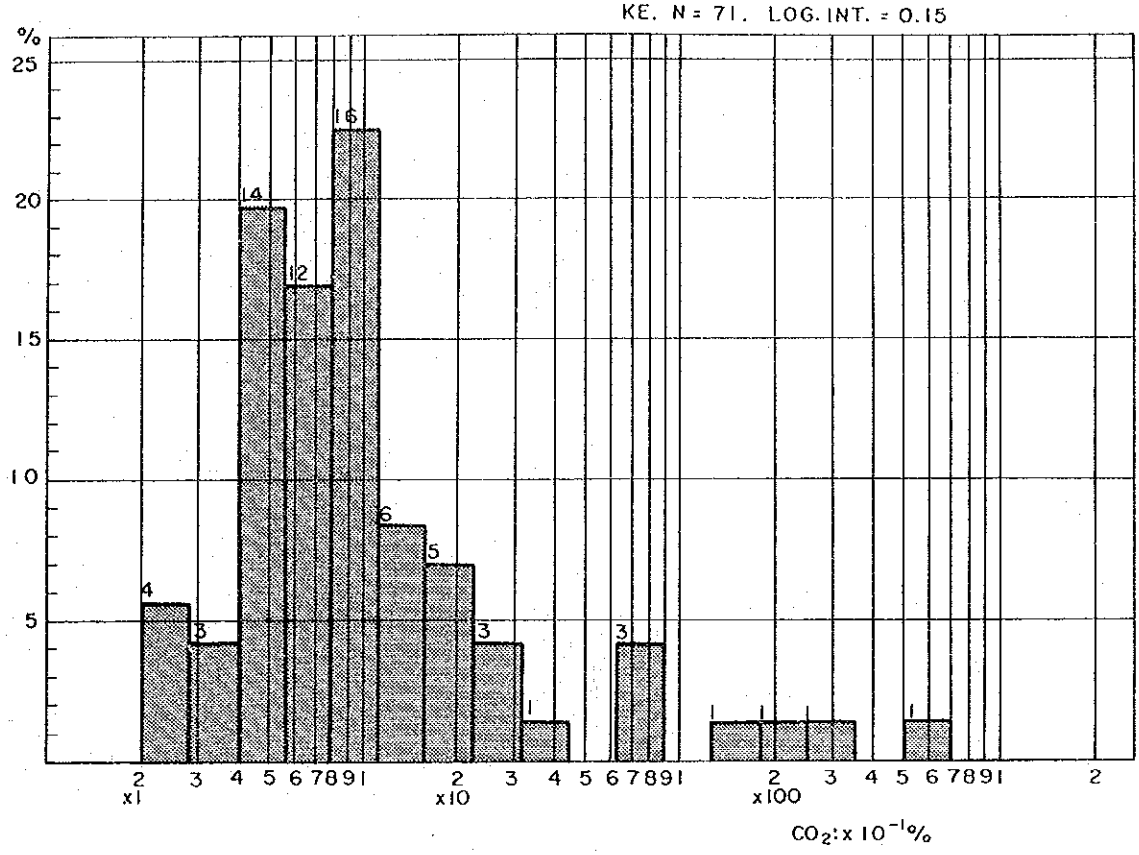

Fig. Ⅲ - 17 CUMULATIVE FREQUENCY DISTRIBUTION (CO_2)

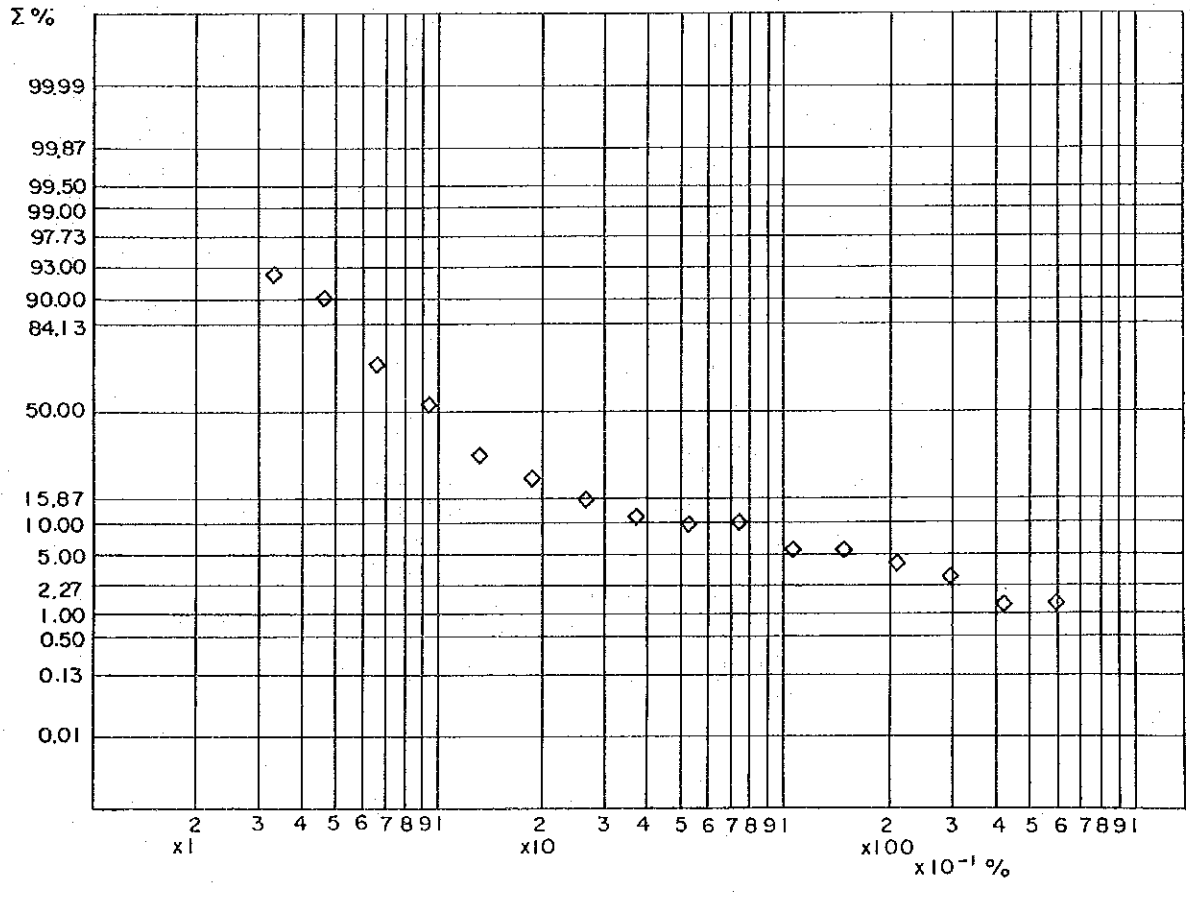

Fig. Ⅲ - 18 HISTOGRAM (HG. Soil)

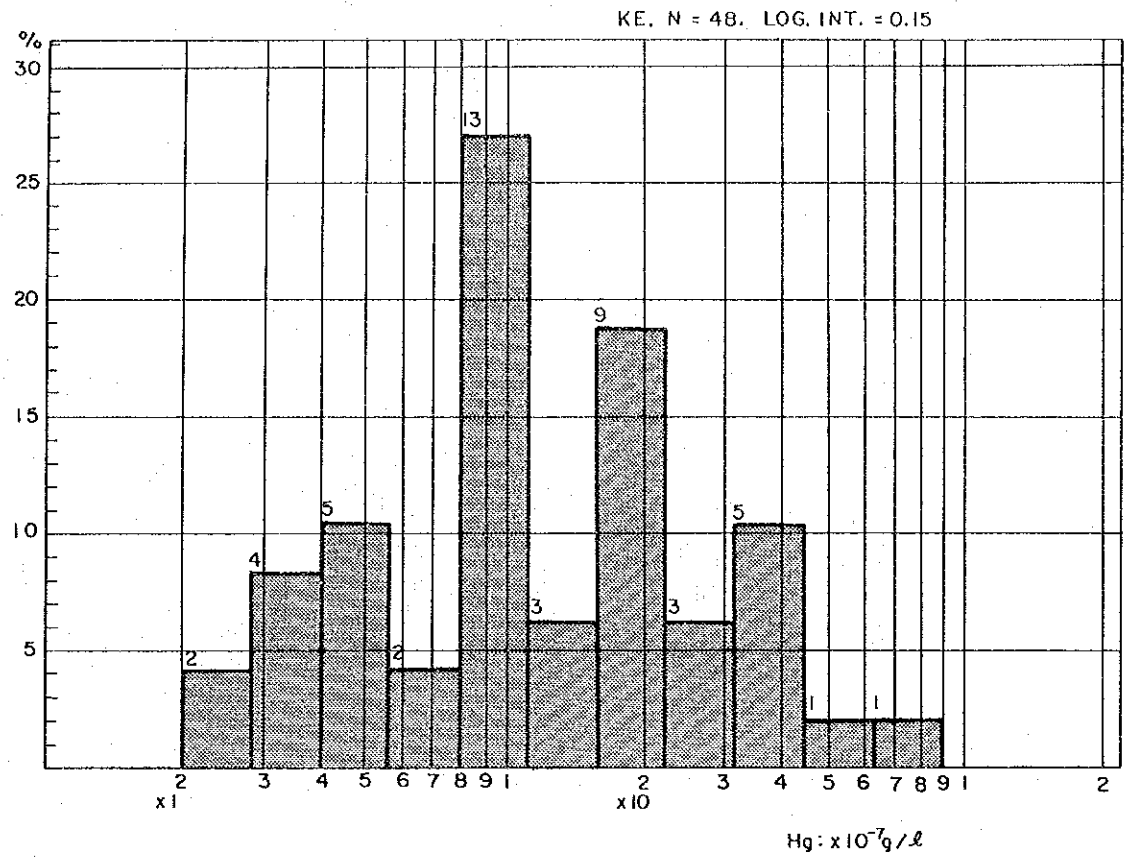

Fig. Ⅲ - 19 CUMULATIVE FREQUENCY DISTRIBUTION (HG. Soil)

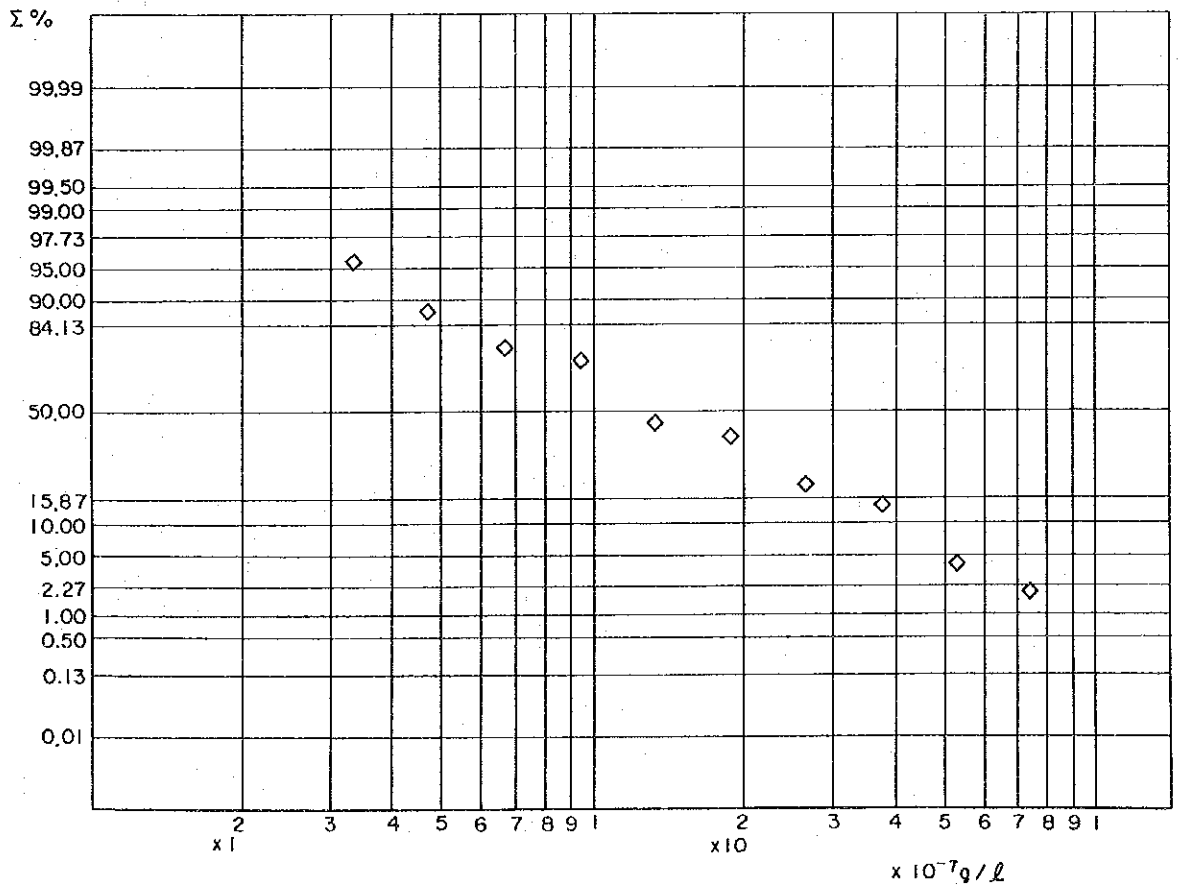

Fig. Ⅲ - 20 HISTOGRAM (Temperature)

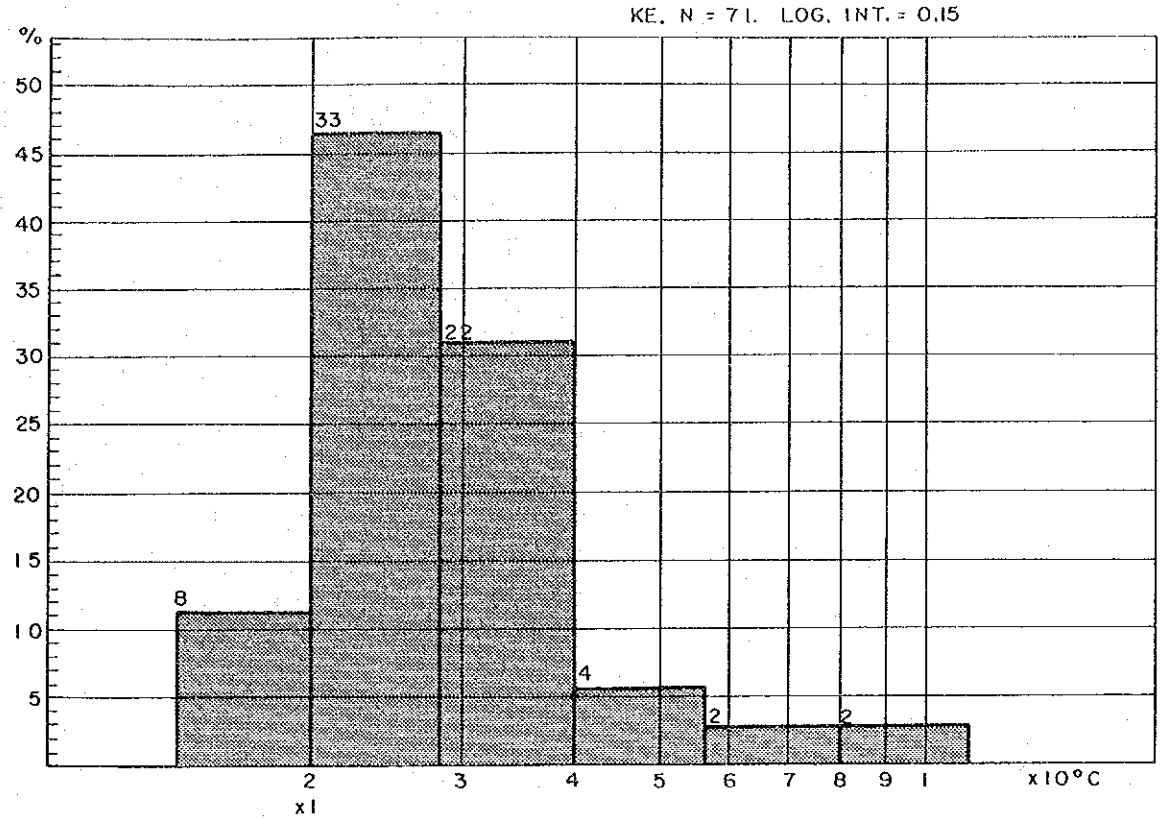

Fig. Ⅲ - 21 CUMULATIVE FREQUENCY DISTRIBUTION (Temperature)

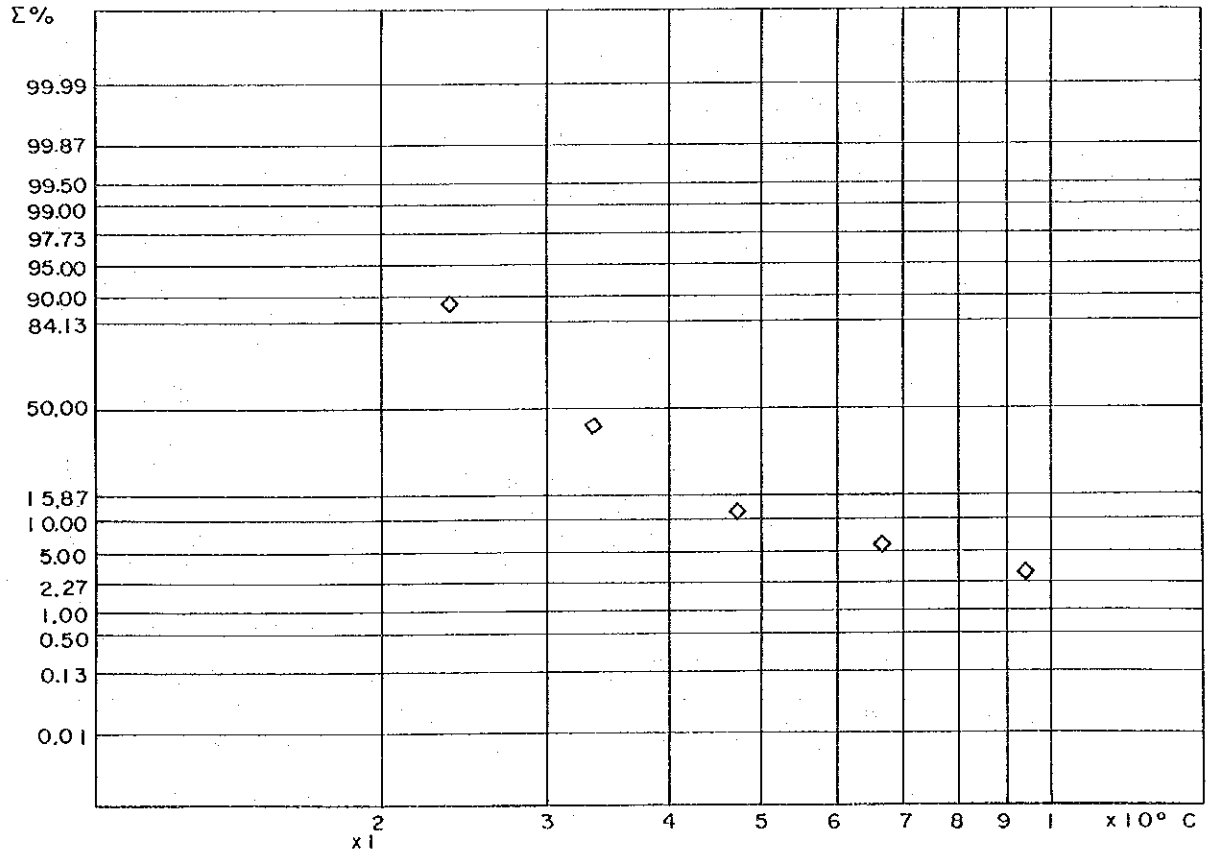

Ⅳ GEOPHYSICAL SURVEY

CHAPTER 1 INTRODUCTION

In the survey area, reconnaissance survey was carried out to study its geothermal potential by UNDP. As the geophysical survey, gravity measurements and galvanic geoelectric sounding by Schlumberger electrode array have carried out.

Gravity survey is to infer underground geological structure, such as faults, geological formation distribution, and intrusive rocks, by studying gravity change.

Electrical survey is to infer underground geological structure by studying electrical resistivity distribution.

Electrical resistivity (called "resistivity" hereafter) of underground rocks highly depends upon it of pore water in rocks. Around geothermal reservoir, underground water is rich in mineral content and high in temperature (Parkhomenko, 1967). Resistivity of water usually becomes lower if temperature is higher and its mineral content is higher (Keller and Frischknecht, 1966). Resistivity of matrix of rocks also becomes lower if temperature is higher. Therefore, resistivity around geothermal reservoir is lower and is usually below 10Ω-m. It is very effective to use electrical prospecting technique for geothermal exploration.

Electrical survey is divided into two categories, the one is horizontal survey to study horizontal geoelectrical distribution, and the other is sounding to study vertical geoelectrical distribution. For the current survey, electrical sounding technique by Schlumberger electrode array is used because it is the same technique as the UNDP survey.

CHAPTER 2 INSTRUMENTATION

Usually geothermal area is a low resistivity zone and a ratio of receiving voltage and transmitting current in resistivity survey becomes smaller in a low resistivity area. In order to collect underground resistivity information in geothermal area, it is important to transmit large electric current into ground. Therefore, for deep electrical survey in geothermal area, effort needs to be put to make contact resistance of current electrodes low and it needs to use large transmitter with large capacity engine generator.

Instruments used for the current survey are written below and are large enough to fulfill the above mentioned requirement. The transmitter can transmit signal with many frequencies and also direct current.

i) Transmitter

Yokohama Electronics Lab.	Model L5202
Maximum Power	800 v, 5A
Frequency	0.1 Hz to 5 Hz and D.C.
Wave Form	Time Domain and Frequency Domain
Weight	50 kg

ii) Engine Generator

Shindaiwa Kogyo	Model 2400
Output Power	2400 vA
Voltage	100 v
Frequency	60 Hz

iii) Recorder

Toa Electronics	Model EPR-100 A
Range	1mv ~100 v, 16 ranges
Accuracy	0.5% (full scale)
Input Impedance	2 M Ω

CHAPTER 3 SURVEY PROCEDURE

There are many kinds of electrode configurations used for geoelectrical sounding techniques. For the current survey Schlumberger electrode configuration is used. The Schlumberger electrode configuration is symmetrical electrode configuration where potential electrodes (P1, P2) and current electrodes (C1, C2) are put symmetric respect to a center (0) of sounding. All points are theoretically in straight line. Electric current is put into ground through two current electrode (C1, C2) and induced electric field is measured between two potential electrodes (P1, P2). Because the wider a current electrodes separation is, the deeper information from the ground can be obtained, measurements are made by making $\overline{(C1\ C2)}/2$ larger while $\overline{(C1\ C2)}/2$ is kept five times more than $\overline{(P1\ P2)}/2$.

For the Schlumberger electrode configuration, an apparent resistivity (ρa) is defined as

$$\rho a = \pi \cdot \frac{\left(\frac{\overline{C1\ C2}}{2}\right)^2 - \left(\frac{\overline{P1\ P2}}{2}\right)^2}{\overline{P1\ P2}} \cdot \frac{V}{I} \quad \cdots\cdots\cdots \qquad (IV-1)$$

where

ρa: apparent resistivity (Ω-m)

V: potential difference (volt)

I : transmitting current (ampere).

In the equation (IV-1), a geometric constant K is defined.

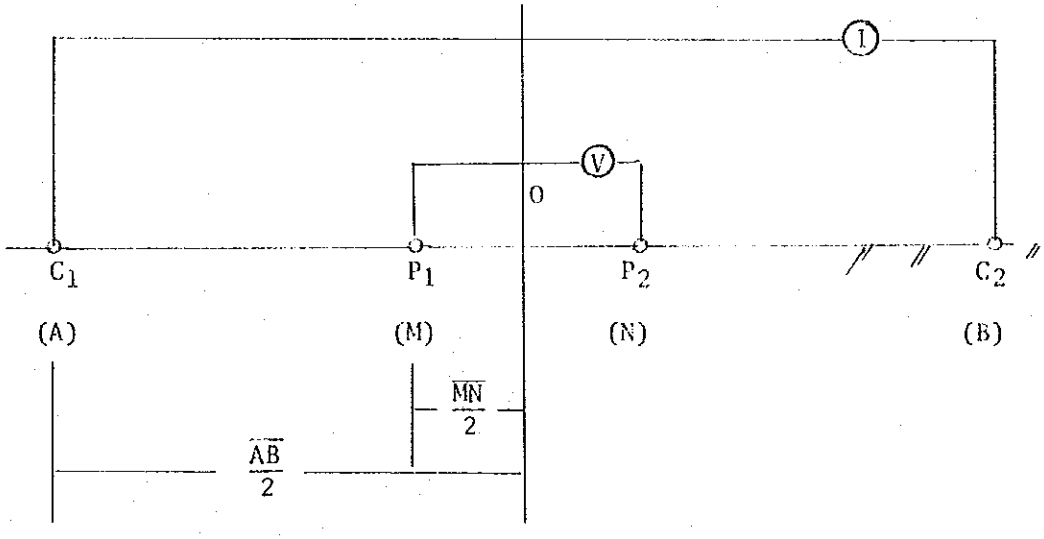

$$K = \pi \cdot \frac{\left(\frac{\overline{C1\ C2}}{2}\right)^2 - \left(\frac{\overline{P1\ P2}}{2}\right)^2}{\overline{P1\ P2}}$$

The equation (IV-1) can be rewritten

$$\rho a = K \cdot \frac{V}{I} \quad \cdots\cdots\cdots\cdots\cdots\cdots \quad (IV\text{-}2)$$

In the equation (IV-2) only the geometric constant depends on electrode configuration.

The combination on current electrode separation $(\frac{\overline{C1\ C2}}{2})$ and potential electrode separation $(\frac{\overline{P1\ P2}}{2})$ used for the current survey is shown in Table IV-1.

Electric current used was transmitted twenty seconds continuously and cut for next five seconds. The skin depth for the transmitted current is over 4,000 meters when resistivity of surface layers is 4Ω-m. Transmitted current and received potential were recorded by a pen recorder. Speed of recording paper was 20 mm/min.

Electric wire with insulating resistance over 3,000 MΩ/km was used for transmission line and connections of wires were very carefully covered. Insulation resistance between transmission wire and the ground was kept extremely high.

Table TV - 1 Combinations of Current and Potential Electrodes

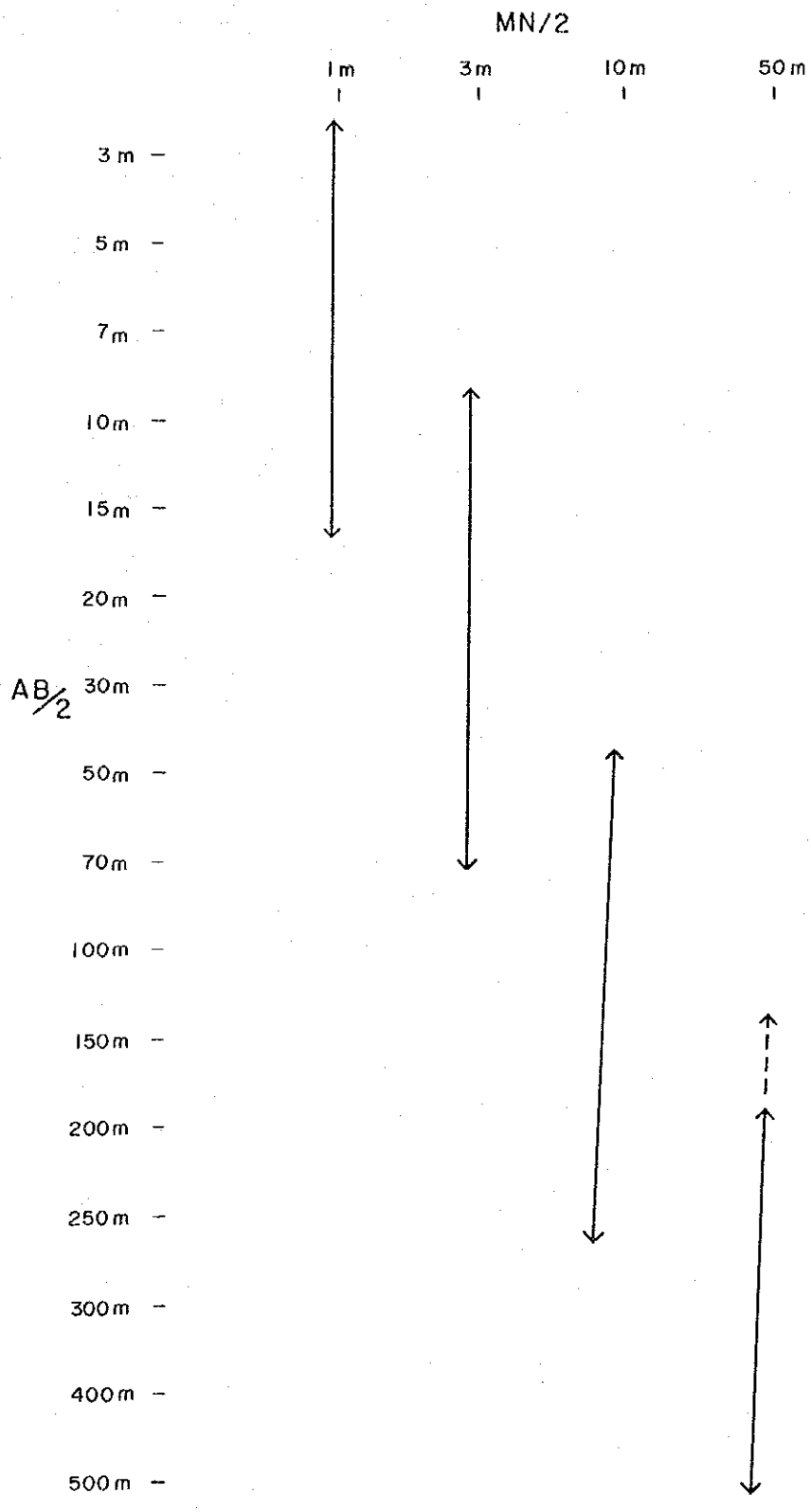

CHAPTER 4 INTERPRETATION

For interpreting Schlumberger geoelectrical sounding data, data were plotted on a log-log graph paper with apparent resistivity along ordinate and half of current electrode separation ($\frac{C1\ C2}{2}$) along abscissa. A drawn curve is called vertical electric sounding curve (VES curve).

The VES curves were interpreted by partial curve matching technique. The partial curve matching uses standard curves of apparent resistivity vs. electrode separation for many resistivity combinations of two layer cases and four types of auxiliary curves (type H, A, K, and Q). The partial curve matching technique is described in many literature, e.g. Keller and Frischknecht (1966), so here it is not explained in details. After interpreting by partial curve matching technique, we calculated theoretical VES curves by using the resistivity layer combination obtained by partial curve matching. If the computer calculated theoretical VES curve did not match well with the field data, we changed either a resistivity or a thickness of interpreted layers and repeated computer calculation until we got satisfactory result.

Data and interpretation process are shown in the following figures and tables.

Field data	Table IV-2-(1) - Table IV-2-(7)
VES curves	Fig. IV-1-(1) - Fig. IV-1-(7)
VES interpretation curves	Fig. IV-2-(1) - Fig. IV-2-(7)
Computer model calculation curves	Fig. IV-3-(1) - Fig. IV-3-(7)